

Long-lived photoexcited states in symmetrical polydicarbazolyldiacetylene

G. Dellepiane, C. Cuniberti, D. Comoretto, G. F. Musso, and G. Figari

Istituto di Chimica Industriale, Università di Genova, Corso Europa 30, I-16132 Genova, Italy

A. Piaggi

Dipartimento di Fisica "A. Volta," Università di Pavia, via Bassi 6, I-27100 Pavia, Italy

A. Borghesi

Dipartimento di Fisica, Università di Modena, via Campi 213/a, I-41100 Modena, Italy

(Received 2 March 1993)

Photoinduced absorption is observed for the polydicarbazolyldiacetylene in the microcrystalline state. The absorption spectrum shows well-defined excitonic features, very similar to those observed for the same polymer in the single-crystal form. Photoexcitation at 2.54 eV gives rise to a structured luminescence emission with the maximum around 1.7 eV. The photoinduced absorption spectrum shows three well-resolved peaks at 0.81, 0.96, and 1.26 eV, a shoulder at 1.04 eV, and a band with a maximum below 0.3 eV. By analyzing the dependence of the photoinduced signals on temperature, laser intensity, phase detection, and chopper frequency, we demonstrate that the long-lived photo-carriers associated with the peaks at 0.81 eV and below 0.3 eV are charged bipolarons. The 0.96- and 1.04-eV bands are tentatively assigned to vibronic excitations of the bipolarons. Moreover, the 1.26-eV band has been assigned here to a triplet exciton transition. The existence of a correlation between the type of long-lived photogenerated defects and the polymer disorder is also discussed.

I. INTRODUCTION

Various conjugated polymers have been studied extensively due to their interesting and potentially useful physical properties. Among these materials, the polydiacetylenes are of particular interest because of their large optical nonlinearities and short excited-state relaxation times.¹⁻⁶ These polymers, which can be obtained as almost defect-free single crystals via solid-state polymerization, ideally behave as wide band-gap monodimensional semiconductors. By varying the substituent groups attached to the conjugated backbone, materials with large differences in optical absorption spectra are produced, but the design of nonlinear optical devices would require detailed knowledge of the corresponding electronic structures.

Photomodulation technique has been widely used to measure photoexcitation energy levels in the gap associated with photogenerated defects. In polydiacetylenes, which possess a nondegenerate ground state, strong electron-phonon interaction leads to self-trapping of the charge into a variety of nonlinear excitations. While excitons are formed by processes involving single-chain excitations, polarons are mainly formed by separation of the electron-hole pair into different chains after interchain diffusion. The subsequent fusion of two positive or negative polarons gives rise to bipolarons.

Different photogenerated defect states (triplet excitons or bipolarons) have been found for polydiacetylenes. Some polydiacetylenes show a single sub-

gap photoinduced absorption,⁷⁻⁹ which has been assigned to a triplet-triplet transition. This interpretation has been further substantiated for the case of poly[1,6-di(toluenesulphonete)-2,4hexadiyne] (PDATS) single crystals on the basis of the magnetic-field dependence of the triplet-state lifetime, measured by time-resolved optical absorption.¹⁰ For other polydiacetylenes, the two sub-gap photoinduced absorption bands observed were shown to be due to charged bipolarons^{11,12} also on the basis of the appearance of infrared-active vibrational modes (IRAV). The formation of bipolaronic defects in these polymers has been further confirmed by measurements of light-induced electron spin resonance (LESR) and/or by the study of the dependence of the photoinduced signals on temperature, pump laser intensity, and modulation frequency.^{12,13}

In this paper we discuss the photoinduced absorption (PA) spectrum of poly[1,6-di(*N*-carbazolyl)-2,4-hexadiyne] (polyDCHD) in the polycrystalline state. Among polydiacetylenes, polyDCHD shows very interesting structural, mechanical, thermal, and optical properties. A substantial redshift relative to other polydiacetylenes is in fact observed of the lowest-energy excitonic optical transition¹⁴ and the photoconductivity action spectrum,¹⁵ and it has been attributed to the increase in the polarizability of the chain environment determined by the carbazolyl substituents.

A careful picture of π - π^* transitions in polyDCHD single crystals has been provided by electric-field-modulated reflectance spectra.^{16,17} These show that the electron states are delocalized along the polymer backbone and

give precise values for the energy gap (2.334 eV) and peak position of the singlet exciton (1.856 eV). According to Sebastian and Weiser,^{16,17} the large binding energy (0.478 eV) and oscillator strength ($f = 0.6$) of the exciton are a consequence of its confinement to the polymer backbone and are closely related to the quasi-one-dimensional character of the π -electron states in this system. Spatial confinement also increases the coupling of the exciton to the continuum states, as revealed from the very large value for the oscillator strength of this transition. On the contrary, the transitions from the ground state into the continuum have very small oscillator strengths.

II. EXPERIMENT

1,6-di(*N*-carbazolyl)-2,4-hexadiyne has been prepared as described in the literature.¹⁵ The monomer was characterized by IR, ¹H NMR spectroscopies, and by elemental analysis. Thermal polymerization was carried out in microcrystalline samples dispersed in KBr pellets at 175 °C following the time evolution of the visible absorption spectrum. No evidence of oligomers as well as of unreacted monomer has been obtained by solvent extracting a microcrystalline sample bulk polymerized in the same experimental conditions.

Electronic absorption spectra were recorded on a Perkin Elmer spectrophotometer model Lambda 9, equipped with the integrating sphere accessory. Photoinduced absorption spectra were obtained on a homemade apparatus. Samples were mounted onto the cold finger of a cryotip Joule-Tomson cryostat (Air Products and Chemicals). The sample temperature was monitored by a thermocouple placed on the cold finger. Transmission (T) spectra were recorded in the range from 0.3 to 2.5 eV with an incident chopped light beam from a tungsten halogen lamp (probe). The transmitted light was dispersed with a McPherson 218 monochromator driven by stepping motor and detected with a photomultiplier tube (visible region) and an InSb detector (infrared region). The output of a EG&G 5205 lock-in amplifier was recorded by using as a reference the frequency of the light chopper. Photoexcitation was provided by the 488-nm line of a cw argon-ion laser (pump). The photoinduced variation in sample transmission ΔT was obtained by chopping the laser light between 1.3 and 900 Hz. ΔT was measured by the lock-in amplifier using as reference the pump chopper frequency. The data, coming from the pump ($-\Delta T$) and probe (T), were stored and processed by an on-line computer in order to obtain the $-\Delta T/T$ spectra.

III. RESULTS AND DISCUSSION

In Fig. 1 the electronic absorption spectrum of polyDCHD in KBr pellets at 300 K shows the prominent transition at 1.92 eV due to singlet exciton accompanied by an apparent vibrational progression which resembles that seen for the same polymer as a single crystal.¹⁴ Also the luminescence exhibits rich vibrational features, as shown in Fig. 2. The first peak of the emission spectrum, measured at 77 K by laser excitation at 488 nm

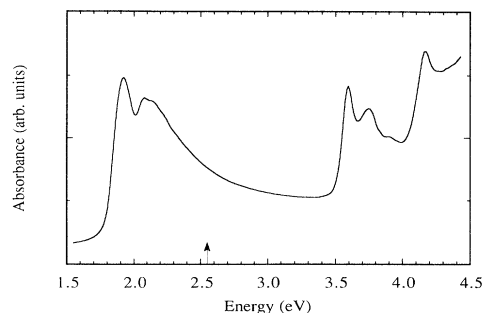


FIG. 1. Electronic absorption spectrum of polyDCHD in KBr pellet at $T=300$ K. The arrow indicates the exciting laser line.

(2.54 eV), i.e., above the band gap of the polymer, falls at 1.75 eV, about 0.17 eV below the singlet exciton absorption. The second, more intense, peak is redshifted by 0.07 eV (≈ 600 cm^{-1}) relative to the first one. It has to be remembered that a vibrational satellite is evident at 680 cm^{-1} to the red of the exciton band in the reflectivity spectrum of polyDCHD single crystals at 77 K.¹⁴

The photoinduced absorption and bleaching at 77 K are reported in Fig. 3(a) for the “in-phase” and in Fig. 3(b) for the “out-of-phase” responses of the lock-in amplifier. These spectra show three sharp and well-resolved peaks at 0.81, 0.96, and 1.26 eV, a shoulder at 1.04 eV, and an indication of a rising band extending into the region below the detection threshold (< 0.3 eV) of our apparatus. In the out-of-phase detection the two signals at 0.81 and 0.96 eV are still observed, even though at much lower intensity, while the 1.26-eV peak disappears. This fact indicates that the lifetime of the defect associated with the last band is shorter with respect to the lifetimes of the lower-energy defects.¹⁸ Notice further that above ≈ 1.6 eV, $-\Delta T/T$ changes sign, indicating a reduction in the strength of the exciton and interband absorptions. This photoinduced bleaching shows superimposed oscillations, whose positions and intensities are strongly dependent on the phase of the detection. Indeed, in the in-phase spectrum two prominent signals appear at ≈ 1.8 and ≈ 2.3 eV, which are the positions of the singlet exciton and energy gap, respectively. On the other hand, with out-of-phase detection, the 1.8-eV signal dominates the bleaching.

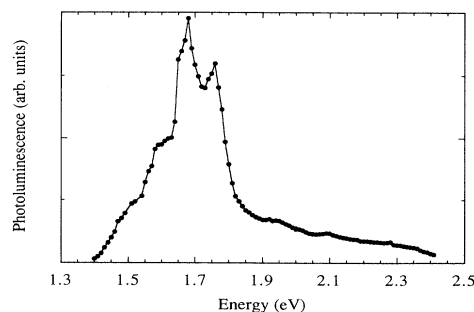


FIG. 2. Luminescence spectrum of polyDCHD at $T=77$ K ($\lambda_{\text{exc}} = 488$ nm, laser power=200 mW).

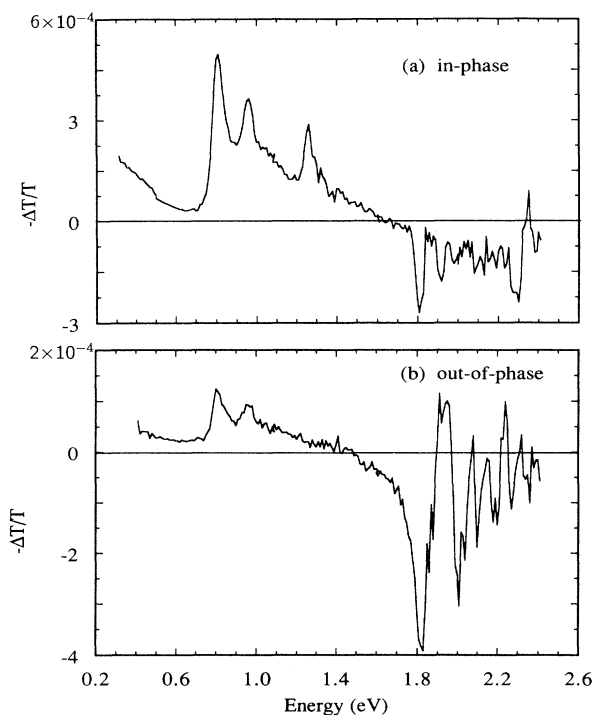


FIG. 3. Photoinduced absorption spectra of polyDCHD for the (a) in-phase and (b) out-of-phase detection, using the 488-nm excitation wavelength, chopper frequency of 13 Hz, $T = 77$ K, and laser power of 200 mW.

To determine the nature of the different photoinduced bands we studied their dependence on temperature, laser power, and chopper frequency. Figure 4 shows the photoinduced spectra at 20 K in the 0.65–1.45 eV region for both the in-phase and out-of-phase detections. We find that the three in-phase PA signals occur at 0.80, 0.95, and 1.24 eV, that is, at slightly lower energy than the ones at 77 K. The intensities of the lowest-energy bands show only marginal changes, while the intensity of the third signal increases by a factor of ≈ 30 on going from 77 K to 20 K. Notice further that the main PA peak at 20 K has a full width at half maximum of 0.05 eV, comparable to those observed for other polydiacetylenes in single-crystal form and that the out-of-phase spectrum still contains no indication of the high-energy peak. The different temperature and phase dependence of the PA response at 1.26 eV with respect to the other two lower absorptions clearly demonstrate that these features have different origin.

The dependences of the 0.81- and 0.96-eV signals and that of the 1.26-eV peak on the laser power I are displayed in Figs. 5 and 6, respectively. While both the lower-energy peaks are observed to behave as $I^{0.5}$, indicating that bimolecular recombination kinetics is dominant under the photoexcitation conditions, a more complex I dependence is exhibited by the 1.26-eV signal. Indeed, in this case, ΔT goes approximately as $I^{0.8}$ for power levels up to about 100 mW and as $I^{0.5}$ for higher laser power. As will be discussed later on, this indicates that both monomolecular and bimolecular recombination

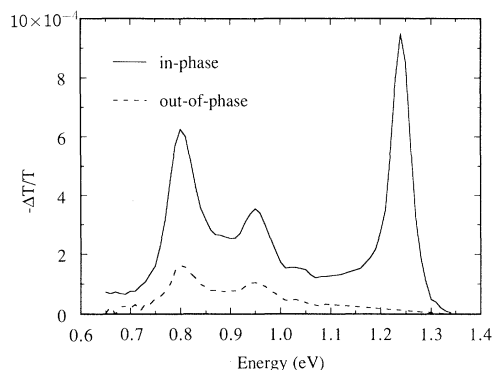


FIG. 4. Photoinduced absorption spectra of polyDCHD for the in-phase and out-of-phase detection at $T=20$ K (other experimental conditions are the same as in Fig. 3).

kinetics are effective for low pump intensity, while the bimolecular kinetics becomes dominant for higher intensity.

The different origins of the energy peaks below and above 1 eV are also revealed by their dependence on chopper frequency. Indeed, at 77 K for both the 0.81- and 0.96-eV peaks a similar $\omega^{-0.3}$ decrease is observed upon increasing the frequency [Fig. 7(a)], while the 1.26-eV photoinduced signal is constant over the whole range of the chopping frequency available [Fig. 7(b)]. At 20 K the latter peak shows constant intensity up to approximately 300 Hz and begins to roll off at higher frequency [Fig. 7(b)].

Hence the results obtained in the present study point to the existence of two different types of photogenerated defects in polyDCHD, one associated with the 1.26-eV band and the other responsible for the 0.81- and 0.96-eV bands. Indeed, there is no doubt on the common origin of these latter peaks as they exhibit a similar dependence on the experimental conditions used.

The interpretation of the PA spectra requires the knowledge of the formation and decay kinetics of the photogenerated defects. Let us first assume that photo-generated carriers decay monomolecularly according to

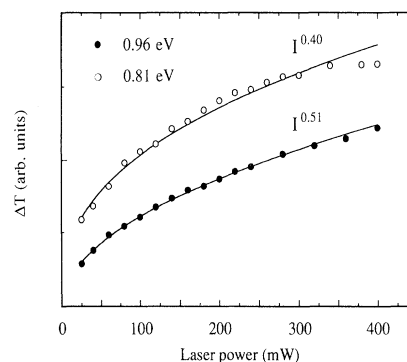


FIG. 5. Laser power dependence of the in-phase photoinduced absorption peaks of polyDCHD at 0.81 eV and 0.96 eV ($\lambda_{\text{exc}} = 488$ nm, chopper frequency of 13 Hz, $T = 77$ K). Lines show the fittings of the experimental data.

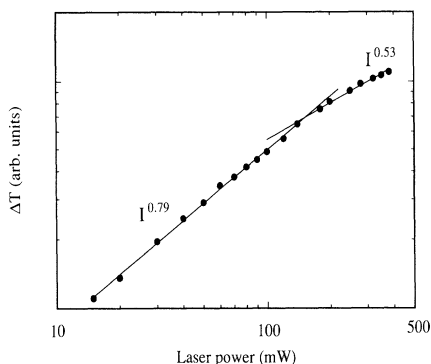


FIG. 6. Laser power dependence of the 1.26-eV photoinduced absorption peak of polyDCHD ($\lambda_{\text{exc}} = 488$ nm, chopper frequency of 13 Hz, $T = 20$ K).

$$\frac{dn}{dt} = G(t) - \gamma n. \quad (1)$$

Here dn/dt is the change in the carrier density per unit time, γ is the inverse lifetime of the carrier ($\gamma = \tau^{-1}$), and $G(t)$ is the pumping term with angular frequency ω , which we model as $gI(\cos \omega t + 1)$, where I is the pump intensity and g the efficiency of the carrier photogeneration. Equation (1) can be exactly solved and its solution for the steady-state case ($t \gg \tau$) is given by

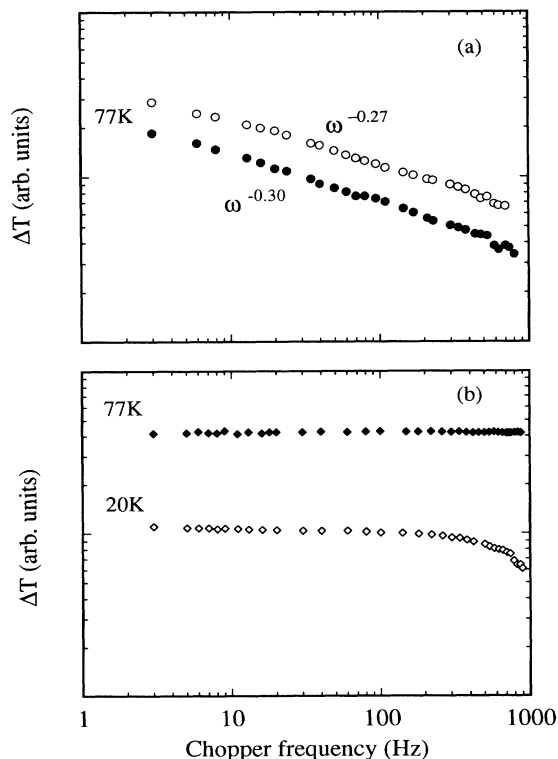


FIG. 7. Chopper frequency dependence of the (a) 0.81-eV (open circle), 0.96-eV (full circle), and (b) 1.26-eV photoinduced signals of polyDCHD ($\lambda_{\text{exc}} = 488$ nm, laser power of 200 mW).

$$n(t) = gI\tau \left[\frac{1}{\sqrt{1 + \omega^2\tau^2}} \cos(\omega t - \phi) + 1 \right], \quad \tan \phi = \omega\tau \quad (2)$$

where ϕ is the phase of the outgoing radiation. From Eq. (2) one derives the photoinduced stationary signal n_s (which is proportional to ΔT):

$$n_s = \frac{gI\tau}{\sqrt{1 + \omega^2\tau^2}}. \quad (3)$$

This well-known equation predicts an I dependence of the PA signals.¹⁸ Moreover, for $\omega\tau \gg 1$, a ω^{-1} law is predicted, while for $\omega\tau \ll 1$ the signal is independent on the chopper frequency. The crossover of the two regions ($\omega\tau \approx 1$) has been used often to obtain an approximate value for τ . Note also from Eq. (2) that $\phi \rightarrow 0$ for very small values of the lifetime and $\phi \rightarrow \pi/2$ for very large values of τ . The in-phase ($\phi = 0$) and out-of-phase ($\phi = \pi/2$) photoinduced spectra can be, and have been, used to detect states with different lifetimes.

In the case of a quadratic recombination, the kinetics equation is given by

$$\frac{dn}{dt} = G(t) - \beta n^2. \quad (4)$$

Note that now (in contrast to the linear recombination kinetics) we cannot introduce a lifetime independent of the light intensity with a constant value during the whole relaxation process. In fact the relaxation process has an infinite number of values of τ , but one of them has a special meaning, the lifetime under steady-state conditions τ_s .

Although Eq. (4) cannot be exactly solved for the periodic form of $G(t)$ considered above, a solution can be given by approximating the modulation term G with a symmetric square light wave.¹⁹ The following expression is obtained for the steady-state photoinduced signal:

$$n_s = \frac{N\alpha \tanh \alpha}{\alpha + \tanh \alpha} \quad (5)$$

where $N = \sqrt{gI/\beta}$, $\alpha = \pi/(\omega\tau_s)$, and $\tau_s = 1/\sqrt{gI\beta}$.

For large values of α ($\omega\tau_s \ll 1$), $n_s \rightarrow N\alpha/(1+\alpha) \approx N$, i.e., the photoinduced signal is independent of ω and shows a square-root dependence on the laser intensity. On the contrary, for small values of α ($\omega\tau_s \gg 1$) the signal approaches zero as $N\alpha$, that is, with a ω^{-1} dependence on the chopper frequency. The dependence on the laser intensity is linear. The crossover region from low to high chopper frequencies depends on the laser intensity in agreement with experimental data.¹³ We want to stress here that the comparative analysis of the predictions of Eqs. (3) and (5) allows us to assign the type of recombination process by means of the dependence of the PA signals in the low-frequency limit ($\omega\tau \ll 1$, $\omega\tau_s \ll 1$) as well as of the crossover region on the laser intensity. Instead, in the high-frequency limit the kinetics of the monomolecular and bimolecular processes are indistinguishable.

Finally, by using the same method reported in Ref. 19, we have derived an expression for the photoinduced signal in the case where both monomolecular ($-\gamma n$) and bimolecular ($-\beta n^2$) decays are operative. The following

relationship has been obtained:

$$n_s = \frac{gI \tanh \frac{\gamma\pi}{2\omega} \tanh \frac{P\pi}{\omega}}{\frac{\gamma}{2} \tanh \frac{P\pi}{\omega} + P \tanh \frac{\gamma\pi}{2\omega}} \quad (6)$$

where $\gamma = \tau^{-1}$, $P = \sqrt{\beta g I + \gamma^2/4} = (2\tau)^{-1} + (\tau_{s'})^{-1}$, and $\tau_{s'}$ is the lifetime of the bimolecular component of the whole relaxation process under steady-state conditions. Equation (6) collapses into Eq. (5) for the particular case $\gamma = 0$ ($\omega\tau \rightarrow \infty$), while for $\beta = 0$ ($\omega\tau_{s'} \rightarrow \infty$) it predicts the same intensity and frequency dependence as Eq. (3), although it is formally different. The lifetime of the whole process, which originates the PA signal described in Eq. (6), is given by $\tau_t^{-1} = \tau^{-1} + \tau_{s'}^{-1}$. Under the condition of both $\omega\tau_{s'} \ll 1$ and $\omega\tau \ll 1$ Eq. (6) becomes

$$n_s = \frac{\gamma}{2\beta} [\sqrt{1 + 4\beta g I \gamma^{-2}} - 1]. \quad (7)$$

From this equation the PA signal is predicted to be independent of the chopper frequency and increasing with the laser intensity, with a changeover from the I to $I^{0.5}$ dependence when the bimolecular regime becomes dominant. For both $\omega\tau_{s'} \gg 1$ and $\omega\tau \gg 1$ the signal varies linearly with the laser intensity and decreases following a ω^{-1} law.

These predictions allow us to give an interpretation of the data discussed above and to propose the following assignment. First of all we propose to assign both the structured band around 0.8 eV and the rising band below 0.3 eV to bipolaronic transitions, consistently with previous assignment in polycarbazolydiacetylenes (Ref. 13) and according to the behavior of the two peaks at 0.81 and 0.96 eV in terms of temperature, laser intensity, chopper frequency, and phase detection. Such a detailed analysis could not be performed on the low-energy band, which qualitatively follows the behavior of the higher-energy component, because of its low intensity in the range accessible to our apparatus. Moreover, for the reasons discussed below we consider the sharp, well-defined peak at 0.96 eV as due to a vibronic satellite of the 0.81-eV signal. We believe that also the 1.04-eV shoulder may be considered as evidence of a higher-energy vibronic satellite.

Vibronic structures in bipolaronic bands have been observed in other conjugated polymers such as, for instance, in poly(*p*-phenylene-vinylene) (PPV),¹⁸ and it is conceivable that these structures, where nonevident, might be hidden underneath the broad signals usually presented by bipolarons. It has to be remarked that vibronic satellites of the singlet exciton are evident in the absorption spectra of both polyDCHD and PPV. Moreover, the bleaching in the PA spectra of our samples shows clear evidence of the involvement of the singlets in the photogeneration of the long-lived defect states discussed here. A vibronic structure of a photogenerated defect state has been observed also in the optical transition of the neutral soliton level in trans-polyacetylene.²⁰

The temperature dependence of the 0.81- and 0.96-eV bands, small in comparison to that of the 1.26-eV signal, is similar to that observed for bipolarons in poly-

carbazolydiacetylenes and in other conjugated polymers. The behavior with the laser intensity is also consistent with a bimolecular relaxation process of long-lived bipolarons. The long lifetime of the states associated with bipolarons is revealed in both the phase and chopper frequency dependence of the PA signals. In fact, the $\omega^{-0.3}$ decrease of the signal amplitudes indicates that the structured band dominates the photoinduced spectrum at long times, consistent with the long-time PA spectrum observed in preliminary measurements carried out in a Fourier transform infrared spectrometer.²¹ The $\omega^{-0.3}$ dependence, as well as that measured in several conjugated polymers,^{18,22} is in disagreement with the predictions of Eq. (5). This discrepancy has been commonly interpreted in terms of a broad range in excited-state lifetimes due to a distribution in defect trapping depths.

As to the 1.26 PA band, whose origin is less clear, experimental evidence points to the photogeneration of a subgap defect with a lifetime shorter than that of the bipolaronic states. An evaluation of its lifetime, as obtained from the chopper frequency dependence, gives a value somewhat smaller than 1 ms at 20 K and a substantially lower value at 77 K, in agreement with the large temperature effect on the photoinduced signal. The laser intensity dependence rules out the photocreation of defects with a simple monomolecular decay. On the other hand, this absorption cannot be attributed to the photocreation of polarons and bipolarons, which are expected to recombine bimolecularly. In this case Eq. (5) predicts an inverse square-root dependence of the lifetime with the laser intensity. Therefore, it turns out that a change from an I to $I^{0.5}$ dependence would require a variation in the lifetimes with the laser intensity so as to allow the shift from the high- to the low-frequency limit upon increasing I . At a chopper frequency of 13 Hz, using the definition of τ_s and the 1-ms value derived above for the lifetime at 200 mW, it can be inferred that $\omega\tau_s \ll 1$ in the whole range of the available laser power.

We are therefore left with the possibility that triplet excitons are formed in this polydiacetylene and that the 1.26-eV signal results from a triplet-triplet transition, in agreement with previous findings in other polydiacetylene single crystals. The observed laser intensity dependence may in fact indicate the presence of both monomolecular and bimolecular decays. This is consistent with excited-state spontaneous relaxation of the triplet exciton and bimolecular annihilation processes of triplet excitons as observed in many organic molecular crystals²³ and according to the behavior discussed above in Eq. (6). Notice further that the millisecond lifetime of this excitation implies that the radiative transition to the ground state is not dipole allowed, in agreement with our assignment. A decay through both the monomolecular and bimolecular channels has been also proposed for the triplet excited state in the 1.3–1.5 eV region in PDA-TS single crystals on the basis of the laser intensity dependence of the photoinduced reflectance.²⁴

In summary, the photoinduced spectrum of polyDCHD shows a variety of features which we attribute to both bipolaronic bands and to a triplet excitonic transition. The presence of charged bipolarons has been further con-

TABLE I. The values of U_{eff} and Γ (for the BK and CR models) calculated from the experimental values of the energy gap and the bipolaron transitions for several PDA's.

	E_g (eV)	$\hbar\omega_1$ (eV)	$\hbar\omega_2$ (eV)	$2\hbar\omega_0$ (eV)	U_{eff} (eV)	Γ_{BK} (eV)	Γ_{CR} (eV)
PolyCPDA	2-2.2	0.45	1.1	0.65	0.21-0.31	0.11	1.0
PolyDCHD	2.335	0.1	0.8	0.7	0.71	0.10	1.0
PDA-1OH	2.4	0.25	1.325	1.075	0.41	0.23	1.2

firmed by the appearance of IRAV modes in preliminary photoinduced absorption measurements in the infrared region.²¹ No LESR nor absorption-detected magnetic resonance²⁵ experiments have been performed so far on this polymer. Hence the assignment of the 1.26-eV signal to the triplet exciton, even though reasonable on the basis of all the data here discussed, cannot be unambiguously given without the support of spin-dependent photogeneration measurements.

At this point, we would like to add a few comments on the existence of a correlation between the nature of the photogenerated defects and the degree of disorder in the crystal structure which derives from chain disorder. Such a correlation may help in clarifying the different photoinduced spectra exhibited by different polydiacetylenes in terms of structural disorder. Indeed, it has been experimentally observed in other conjugated polymers that the formation of bipolaronic defects is strictly associated with the presence of structural defects in the polymer chain. In contrast to the three photoinduced signals found in "ordinary" PPV (Ref. 18) and in film of poly[2-methoxy, 5-(2'-ethyl-hexyloxy)-*p*-phenylene vinylene] (MEH-PPV) (Ref. 26) the steady-state photoinduced absorption spectra of both improved PPV (Ref. 27) and MEH-PPV/polyethylene blends²⁶ show only one subgap absorption near 1.4 eV, assigned to the triplet-triplet transition. A similar explanation could be given to the fact that some photoexcited polydiacetylenes give rise to a single high-energy peak around 1.4 eV, while others exhibit two bipolaronic absorptions. In our sample, where evidence of an ordered structure is derived from the prominent exciton absorption, the PA spectrum exhibits three peaks, in contrast to previous findings on other polycarbazolyldiacetylenes characterized by broad absorption spectra, for which only bipolarons were detected.

We now compare the electronic properties of polyDCHD with those of other PDA's, in relation to the long-lived photoinduced signals associated with bipolarons. The present data do not allow us to assign the low-energy peak of the bipolaron in polyDCHD to a precise frequency value as remarked above. However, a value around 0.1 eV can be inferred from the analysis of the photoinduced infrared spectrum.²¹ The energy separation of the two bipolaronic peaks ($2\omega_0$) in polyDCHD would thus result as 0.7 eV, i.e., of the same order of magnitude of that found for poly[1-(*N*-carbazolyl)penta-1,3-diyne-5-acetoxy] (polyCPDA) (Ref. 13) and much smaller than that reported for poly(1-methyl penta-1,3-diyne-6-ol) PDA-1OH (Ref. 11) (see Table I).

The size of the bipolaron is determined by the con-

finement parameter Γ , which is a function of the ratio $2\omega_0/E_g$, where E_g is the energy gap. By using the Brazovski-Kirova (BK) model²⁸ we derive for polyDCHD a value $\Gamma = 0.1$, which is comparable with that obtained for polyCPDA, but much smaller than that for PDA-1OH (see Table I). The same behavior, but with values of Γ substantially higher (Table I), is obtained by using the very recent model proposed by Choi and Rice (CR) (Ref. 29) which accounts for the superalternant structure of the polydiacetylenes not included in the BK model. Though the physical picture derived from the two different models is opposite (weak confinement of the bipolarons in the BK model, strong confinement in the CR model), they agree on the prediction that Γ for polyDCHD is similar to that for polyCPDA and both are lower than the value found for PDA-1OH.

We note that the introduction of carbazolyl substituents appears to reduce the degree of confinement of the photoinduced defects, independently on the details of the chemical structure such as the number of the carbazolyl groups and the mode of attachment to the polymer skeleton. Furthermore it has to be noted that the values of Γ do not appear to depend on the degree of chain order as evidenced by the differences in the electronic absorption spectra.

For a bipolaron, in the presence of Coulomb interaction, the sum of the transition energies ω_1 and ω_2 can be related to the band gap through the relationship³⁰

$$\omega_1 + \omega_2 = E_g - 2U_{\text{eff}} \quad (8)$$

where U_{eff} is proportional to the effective Coulomb energy in the Hubbard on-site model. Since we have $\omega_1 + \omega_2 = 0.9$ eV, we find $U_{\text{eff}} = 0.7$ eV, which is even larger than the value 0.41 estimated for PDA-1OH. We can conclude by noting that the electron correlation appears to be even larger in polyDCHD than the still large values calculated for other polydiacetylenes. On the other hand, the electron-phonon coupling in this system is so large as to forbid the discussion of the experimental data in terms of the electron-electron interaction. Theoretical calculations including both strong electron-phonon and electron-electron interactions are needed to allow quantitative interpretation of the experiments in these semi-conducting organic materials.

ACKNOWLEDGMENTS

We acknowledge support by the Italian Ministry of University and Scientific and Technological Research (MURST) and by the National Research Council (CNR).

- ¹D.J. Sandman, G.M. Carter, Y.J. Chen, B.S. Elman, M.K. Thakur, and S.K. Tripathy, in *Polydiacetylenes*, edited by D. Bloor and R.R. Chance (Nijhoff, Dordrecht, 1985), p. 299.
- ²*Organic Materials for Non-linear Optics*, edited by R.A. Hann and D. Bloor (The Royal Society of Chemistry, London, 1989).
- ³P.A. Chollet, F. Kajzar, and J. Messier, *Synth. Met.* **18**, 459 (1987).
- ⁴K. Ichimura, T. Kobayashi, H. Matsuda, H. Nakanishi, and M. Kato, *J. Chem. Phys.* **93**, 5510 (1990), and references therein.
- ⁵T. Kobayashi, M. Yoshizawa, U. Stamm, M. Taiji, and M. Hasegawa, *J. Opt. Soc. Am.* **78**, 1558 (1990), and references therein.
- ⁶S. Etemad and Z.G. Soos, in *Spectroscopy of Advanced Materials*, edited by R.J.H. Clark and R.E. Hester (Wiley, New York, 1991) p. 87, and references therein.
- ⁷J. Orenstein, S. Etemad, and G.L. Baker, *J. Phys. C* **17**, L297 (1984).
- ⁸S. Etemad, G.L. Baker, J. Orenstein, and K.M. Lee, *Mol. Cryst. Liq. Cryst.* **118**, 389 (1985).
- ⁹T. Hattori, W. Hayes, and D. Bloor, *J. Phys. C* **17**, L881 (1984).
- ¹⁰L. Robins, J. Orenstein, and R. Superfine, *Phys. Rev. Lett.* **56**, 1850 (1986).
- ¹¹F.L. Pratt, K.S. Wong, W. Hayes, and D. Bloor, *J. Phys. C* **20**, L41 (1987); *J. Phys. D* **20**, 1361 (1987).
- ¹²Y.H. Kim, M. Novak, Z.G. Soos, and A.J. Heeger, *J. Phys. C* **21**, L503 (1988); *Synth. Met.* **28**, D621 (1989).
- ¹³G. Dellepiane, C. Cuniberti, D. Comoretto, G. Lanzani, G.F. Musso, P. Piaggio, R. Tubino, A. Borghesi, C. Dell'Erba, G. Garbarino, and L. Moramarco, *Phys. Rev. B* **45**, 6802 (1992).
- ¹⁴R.J. Hood, H. Müller, C.J. Eckhardt, R.R. Chance, and K.C. Yee, *Chem. Phys. Lett.* **54**, 295 (1978).
- ¹⁵K.C. Yee and R.R. Chance, *J. Polym. Sci. Polym. Phys.* **46**, 431 (1978).
- ¹⁶L. Sebastian and G. Weiser, *Chem. Phys.* **62**, 447 (1981).
- ¹⁷G. Weiser, *Phys. Rev. B* **45**, 14076 (1992).
- ¹⁸See, for instance, N.F. Colaneri, D.D.C. Bradley, R.H. Friend, P.L. Burn, A.B. Holmes, and C.W. Spangler, *Phys. Rev. B* **42**, 11670 (1990), and references therein.
- ¹⁹D. Comoretto, Ph.D. thesis, University of Genova, 1993; see also S. M. Ryvkin, *Photoelectric Effects in Semiconductors* (Consultants Bureau, New York, 1964).
- ²⁰Z. Vardeny, E. Ehrenfreund, O. Brafman, B. Horovitz, H. Fujimoto, J. Tanaka, and M. Tanaka, *Phys. Rev. Lett.* **57**, 2995 (1986).
- ²¹S. Luzzati, F. Speroni, D. Comoretto, C. Cuniberti, G.F. Musso, and G. Dellepiane (unpublished).
- ²²J. Ruhe, N.F. Colaneri, D.D.C. Bradley, R.H. Friend, and G. Wegner, *J. Phys. Condens. Matter* **2**, 5465 (1990), and references therein.
- ²³J.B. Birks, *Photophysics of Aromatic Molecules* (Wiley-Interscience, London, 1970).
- ²⁴T. Kobayashi and H. Ikeda, *Synth. Met.* **18**, 441 (1987).
- ²⁵X. Wei, B.C. Hess, Z.V. Vardeny, and F. Wüdl, *Phys. Rev. Lett.* **68**, 666 (1992).
- ²⁶L. Smilowitz and A.J. Heeger, *Synth. Met.* **48**, 193 (1992).
- ²⁷K. Pichler, D.A. Halliday, D.D.C. Bradley, R.H. Friend, P.L. Burn, and A.B. Holmes, *Synth. Met.* **55**, 230 (1993).
- ²⁸S.A. Brazovskii and N.N. Kirova, *Pis'ma Zh. Eksp. Teor. Fiz.* **33**, 6 (1981) [*JETP Lett.* **33**, 4 (1981)].
- ²⁹H.Y. Choi and M.J. Rice, *Phys. Rev. B* **44**, 10521 (1991).
- ³⁰D.K. Campbell, D. Baeriswyl, and S. Mazumdar, *Synth. Met.* **17**, 197 (1987).